Effects of the residual ammonium concentration on NOB repression during partial nitritation with granular sludge

Poot, Vincent; Hoekstra, Maaike; Geleijnse, Mitchell A A; van Loosdrecht, Mark C M; Pérez, Julio

DOI
10.1016/j.watres.2016.10.028

Publication date
2016

Document Version
Accepted author manuscript

Published in
Water Research

Link to formal publication Water Research (Elsevier): http://dx.doi.org/10.1016/j.watres.2016.10.028

Effects of the residual ammonium concentration on NOB repression during partial nitritation with granular sludge

Vincent Poot, Maaike Hoekstra, Mitchell A.A. Geleijnse, Mark C.M. van Loosdrecht, Julio Pérez*

Department of Biotechnology, Faculty of Applied Sciences, Delft University of Technology, Van der Maasweg 9, 2629 HZ Delft, The Netherlands

* Corresponding author: julio.perez@uab.es

Abstract

Partial nitritation was stably achieved in a bench-scale airlift reactor (1.5L) containing granular sludge. Continuous operation at 20°C treating low-strength synthetic wastewater (50 mg N-NH_4^+/L and no COD) achieved nitrogen loading rates of 0.8 g N-NH_4^+/(L·d) during partial nitritation. The switch between nitrite-oxidizing bacteria (NOB) repression and NOB proliferation was observed when ammonium concentrations in the reactor were below 2-5 mg N-NH_4^+/L for DO concentrations lower than 4 mg O_2/L at 20ºC. *Nitrospira* spp. were detected to be the dominant NOB population during the entire reactor operation, whereas *Nitrobacter* spp. were found to be increasing in numbers over time. Stratification of the granule structure, with ammonia-oxidizing bacteria (AOB) occupying the outer shell, was found to be highly important in the repression of NOB in the long term. The pH gradient in the granule, containing a pH difference of ca. 0.4 between the granule surface and the granule centre, creates a decreasing gradient of ammonia towards the centre of the granule. Higher residual ammonium concentration enhances the ammonium oxidation rate of those cells located further away from the granule surface, where the competition for oxygen between

AOB and NOB is more important, and it contributes to the stratification of both populations in the biofilm.

Keywords: Stratification; pH gradient; *Nitrobacter*; *Nitrospira*; mainstream conditions.

1. Introduction

Partial nitritation-Anammox processes are currently under development for the treatment of pretreated sewage (Wett, 2007; Lotti et al., 2014a; Gilbert et al., 2014; Wang et al., 2016; Reino et al., 2016). Advantages of these systems compared to the conventional nitrification-denitrification treatment are found in economic and environmental aspects. OPEX and CAPEX for nitritation-Anammox can be reduced because of less aeration and COD requirement, and less sludge production. From the environmental point of view, N_2O and CO_2 emissions can be reduced since these greenhouse gasses are not produced in the Anammox process, whereas they are produced during heterotrophic denitrification (Fux and Siegrist, 2003; Kartal et al., 2010). However, autotrophic nitrogen removal processes in mainstream conditions still cope with some challenges. One of the main problems concerns the process stability in the long term (Winkler et al., 2011; De Clippeleir et al., 2013; Han et al., 2016). Nitrite oxidizing bacteria (NOB) tend to proliferate in long-term partial nitritation operations, affecting the process by oxidising nitrite into nitrate and therefore making the effluent unsuitable for further treatment by autotrophic denitrification by Anammox.

Process control is needed to repress NOB activity and maintain aerobic oxidation of ammonium into nitrite by ammonium oxidising bacteria (AOB). Proposed NOB repression strategies utilize the control of dissolved oxygen (DO) (Blackburne et al., 2008; Lotti et al., 2014b; Ma et al., 2015) or even the DO/ammonium concentrations ratio in the bulk liquid (Bougard et al., 2006; Bartrolí et al., 2010). These strategies are based on the general reported higher oxygen affinity of AOB compared to NOB (Guisasola et al., 2005; Blackburne et al., 2008; Pérez et al., 2009). The lower oxygen affinity of NOB together with the oxygen

limitation imposed in biofilm systems leads to NOB repression (Garrido et al., 1997; Picioreanu et al., 1997; Sliekers et al., 2005; Peng and Zhu, 2006; Pérez et al., 2009; Brockmann and Morgenroth, 2010, among many others). However, Isanta et al. (2015) reported that besides a system operating under oxygen limiting conditions and a higher oxygen affinity for AOB than NOB, a residual ammonium concentration should be maintained in order to keep the growth rate of AOB higher than that of NOB, see Eq. 1. Control of the bulk ammonium concentration influences the ammonium oxidation rate. If Eq. 1 is used to describe the AOB growth rate, then the residual ammonium concentration affects the ammonium saturation term (or Monod term) and therefore controls the growth rate of AOB. Pérez et al. (2014) reported a modelling study in which this concept is used for control of NOB repression. However, until now the influence of the residual ammonium concentration on NOB repression was tested mainly in the long term, to obtain stable partial nitritation in mainstream conditions (Isanta et al., 2015; Reino et al., 2016). No further explanations for the success of the strategy and the repression of NOB have been reported.

$$\mu_{AOB} = \mu_{AOB}^{max}\left(\frac{C_{NH_4^+}}{K_{NH_4^+} + C_{NH_4^+}}\right)\left(\frac{C_{O_2}}{K_{O_2} + C_{O_2}}\right) \quad (1)$$

In this study, a better understanding of the role of the residual ammonium concentration has been pursued. Therefore, instead of aiming to demonstrate the long-term stability of the NOB repression (as done recently at low temperatures in Isanta et al., 2015 and Reino et al., 2016), assessment of the short term effects of the residual ammonium concentration was specifically targeted. Several techniques were used during the research. Batch test experiments, measurements of the hydroxylamine concentration (an intermediate in nitritation), off-gas measurements to monitor NO and N_2O emissions, pH profiles in the granule and FISH on granules slices obtained through cryosectioning were used to investigate the effect of the residual ammonium concentration. Here, we present findings showing the mechanisms that

explain the positive effects of the residual ammonium concentration on NOB repression. These mechanisms are novel and provide explanation to several reported observations for this type of reactors that were poorly understood. The conclusions of the study provide crucial insight in the stability of nitritation and they are very valuable for the next steps in the implementation of anammox in the main water line, to achieve sustainable sewage treatment.

2. Materials and Methods

2.1 Reactor set-up and inoculum

An air-lift reactor with a working volume of 1.5 L was used (Fig. S1). The air flowrate was regulated with a mass flow controller (2 L/min capacity, BROOKS, The Netherlands). DO and pH were measured but not controlled.

The granular sludge was originally obtained from the sidestream reactor in WWTP Olburgen, The Netherlands(Abma et al., 2010). The reactor is performing one-stage nitrogen removal through partial nitritation/anammox process. However, a period of acclimation (ca. two months) of the sludge to mainstream conditions was carried out in the pilot plant of the LIFE project CENIRELTA (Cost Effective NItrogen REmoval by Low-Temperature Anammox) in the WWTP Dokhaven (The Netherlands). The pilot plant treats wastewater obtained from a large part of Rotterdam (south, east, centre) after COD removal in a highly loaded aerobic COD removal reactor or A-stage (see a description in Lotti et al., 2014a). When the inoculum was obtained, the effluent concentrations in the CENIRELTA pilot plant were 21 ± 2 mg N-NH_4^+/L, 0.6 ± 0.3 mg N-NO_2^-/L, 7 ± 1 mg N-NO_3^-/L and ca. 45 mg COD/L at 23±1 °C.

The reactor inoculum was 1 L, containing 4 gVSS/L. Initial maximum activity tests yielded 29 ± 3 mg N-NO_2^-/(gVSS·d) for AOB, 56 ± 7 mg N-NO_3^-/(gVSS·d) for NOB and 21 ± 0.6

96 mg $N\text{-}NH_4^+$/(gVSS·d) for AMX. At the day of inoculation, the average granule diameter was
97 ca. 0.9 mm.

98

99 **2.2 Wastewater**

100 Synthetic wastewater was used containing (per litre of tap water) 0.73 g K_2HPO_4, 0.104 g
101 KH_2PO_4, 1.26 g $NaHCO_3$, 0.236 g $(NH_4)_2SO_4$, 0.25 mL Fe^{2+}-solution and 0.12 mL trace
102 elements solution. The Fe^{2+}-solution consisted of (per litre demineralised water) 6.37 g EDTA
103 and 9.14 g $FeSO_4 \cdot 7H_2O$, and the pH was adjusted to 2.5. The trace elements solution
104 contained (per litre Milli-Q water) 19.11 g EDTA, 0.43 g $ZnSO_4 \cdot 7H_2O$, 0.24 g $CoCl_2 \cdot 6H_2O$,
105 1.0 g $MnCl_2 \cdot 4H_2O$, 0.25 g $CuSO_4 \cdot 5H_2O$, 0.22 g $(NH_4)_6Mo_7O_{24} \cdot 4H_2O$ (=1.25 mM Mo), 0.20 g
106 $NiCl_2 \cdot 6H_2O$, 0.09 g $HNaSeO_3$, 0.014 g H_3BO_3 and 0.054 g $Na_2WO_4 \cdot 2H_2O$. The pH was
107 adjusted to 6 with solid NaOH.

108

109 **2.3 Reactor operation**

110 The reactor was operated in continuous mode at atmospheric pressure and temperature was
111 controlled at 20°C. At this temperature the advantage of AOB compared to NOB in terms of
112 the maximum specific growth rate is assumed to be rather small (Hunik et al., 1994; Hellinga
113 et al., 1998). The inflow rate was controlled manually (in the range 8-20 L/d) to explore the
114 role of the residual ammonium concentration in both the short and long term. During the
115 continuous operation the reactor pH was rather constant at 7.7 ± 0.1.

116 The reactor operation has been divided into 5 phases (Fig. 1). For details of the pseudo-steady
117 states achieved see Table 1.

118

Calculation of specific ammonium oxidation and nitrate production rates

To calculate specific rates, the biomass concentration was linearly interpolated and the accumulation term was also taken into account, to have a better estimation during transient states. For the accumulation term, the first derivative of the (ammonium or nitrate) concentration in time was approached by the incremental ratio: $^{dC}/_{dt} \cong {}^{\Delta C}/_{\Delta t}$.

Diameter distribution

The diameter distribution of the granules was measured with the aid of image analysis following the method described in Tijhuis and van Loosdrecht (1994). Surface-based average diameter of the granules was obtained and number of granules and size distribution histograms are detailed in the supplementary information for each one of the measurements.

Batch tests

The batch tests were performed in the same (airlift) reactor used for the continuous operation. Continuous operation was stopped and an ammonium pulse was added. During the batch test the DO and pH were not controlled. For the Anammox batch test the reactor was switched from sparging air to supplying nitrogen gas to obtain anaerobic conditions. When the DO was 0%, the medium flowrate was stopped and samples were withdrawn from the top section of the reactor.

2.4 Analytical procedures

Ammonium, nitrite and nitrate concentrations were measured offline with Hach Lange cuvette kits. Dry weight (TSS), ash content and volatile suspended solids (VSS, dry weight minus ash content) were determined according to standard methods (APHA, 2012). Hydroxylamine concentrations were measured using a colorimetric method (Frear and Burrell, 1955),

following an *ad hoc* procedure for sample preparation described in Soler-Jofra et al. (2016). N_2O and NO off-gas concentrations were periodically measured online with a Servomex 4900 infrared gas analyser.

2.5 Fluorescence In Situ Hybridization (FISH)

For analysis of the microbial population, the granules were pottered, washed, fixed and loaded onto with gelatine pre-coated Teflon slides according to the procedure described in (Third et al., 2001). For cryosectioning of the granules, the granules were washed (3h) in 1x PBS before being fixed (1h). Teflon slides were coated with 0.01% poly-L lysine solution. Granules were put in freeze-medium and cut with a freeze-microtone (Leica CM 1990) at -25°C. The obtained slices (10-15 µm thick) were placed on the pre-coated slides and washed with 50% ethanol solution for 5 minutes, to remove the freeze-medium and regain hydrophobicity. Probe hybridization to both pottered samples and cryosectioned slices was again performed as described in (Third et al., 2001). Oligonucleotide probes used are listed in Table S1. Image analysis was done with a Zeiss Axioplan 2 Imaging microscope, together with an AxioCam MRm camera (Zeiss), an ebq100 lamp for fluorescent light and the Axiovision software.

2.6 pH profile in the granular sludge

To determine the pH profile, a granule was fixed in the middle of a flow chamber with a small steel clip (see also the supplementary information, section S1.3). Medium was sparged with air and pumped from the bottom to the top. For the measurements of the pH difference between bulk liquid and granule inside, the pH microelectrode was placed closely above the granule. The pH of the bulk liquid was measured, followed by 1 step of 1000 µm, to measure

the pH inside the granule. The complete experiment was performed at ammonium concentrations of 49 and 11 mg N/L (a different granule was used for each ammonium concentration).

3. Results

3.1 Reactor operation

During the entire operation period (223 days) the wastewater inflow rate was used as manipulated variable to control the residual ammonium concentration (Fig. 1A). However, also the inflow ammonium concentration was lowered from 50 to 40 mg N-NH_4^+/L during phase II (Fig. 1D). The entire performance was divided into 5 phases (Fig. 1), and achieved pseudo-steady states are summarized in Table 1.

Phase I

The start-up period (days 0-11 in phase I, phase I: day 0-67) was used for adaptation of the biomass and partial nitritation-Anammox was targeted. Nevertheless, the Anammox activity decreased very fast and eventually was totally lost (see details in section 3.4). As a consequence, nitrite built up in the effluent and the reactor was mainly performing nitritation. From day 50 onwards, the single targeted process was nitritation. The airflow rate was increased step wise to reach a higher DO concentration in the range of 0.7-0.8 mg O_2/L (Fig. 1C). During days 53 to 67 a pseudo-steady state was reached with reactor and effluent concentrations of 16 ± 1 mg N-NH_4^+/L, 24 ± 2 mg N-NO_2^-/L, 6 ± 1 mg N-NO_3^-/L and 0.7 ± 0.1 mg O_2/L. This indicates that nitritation was the main process taking place, NOB repression was efficient, although still some residual nitrite oxidation was present. To test the influence of residual ammonium in NOB repression, in a next phase the effluent ammonium concentration was decreased.

Phase II

In phase II (days 68-139) the reactor contained low bulk ammonium concentrations, with an average of ca. 2 mg N-NH_4^+/L. This was obtained by the decrease in the inflow ammonium concentration from 50 to 40 mg N- NH_4^+/L (Fig. 1D). Immediately after the step-down in residual ammonium concentration the nitrate concentration increased (Fig. 1E), although there was not a complete switching towards nitrification, and nitrite was still at high values (ca. 25 mg N/L). During days 127 to 137, the residual ammonium concentration decreased and the system switched from oxygen limitation to ammonium limitation resulting in the complete oxidation of ammonium into nitrate (i.e., nitrification). The stoichiometry of the nitrification process makes that 3.43 g O_2/g N-NH_4^+ are required for the oxidation of ammonium to nitrite and 4.57 g O_2/g N-NH_4^+ is required for the complete oxidation of ammonium to nitrate. By taking into account ammonium and oxygen diffusivities (Picioreanu et al., 1997), the threshold value for the switch from oxygen-limitation to ammonium-limitation could be calculated using Eq. 2 (Harremoes, 1982; Bartrolí et al., 2010).

$$\frac{C_{O_2}}{C_{NH_4^+}} < \frac{\gamma_{O_2/N-NH_4^+} D_{NH_4^+}}{\mathrm{D}_{O_2}} = \frac{3.43 \times 1.9 \times 10^{-4}}{2.2 \times 10^{-4}} = 3.0 \ \frac{gO_2}{gN} \qquad (2)$$

During the last part of phase II the values of the DO/ammonium concentrations ratio exceeded 3.0 g O_2/g N, meaning the switch from oxygen limitation to ammonium limitation (Fig. 1B). Due to ammonium limitation, the ammonium oxidation rate decreased and the DO concentration increased. For days 117-139 a pseudo-steady state was reached with concentrations of 0.8 ± 0.3 mg N-NH_4^+/L, 24 ± 11 mg N-NO_2^-/L, 14 ± 11 mg N-NO_3^-/L and 1.7 ± 1.0 mg O_2/L. When bulk ammonium concentration reaches such low values, NOB repression is not possible, and therefore most ammonium is converted to nitrate.

Phase III

In the beginning of phase III (phase III: day 140-168) the bulk ammonium concentration was increased to ca. 12 mg N/L. The system switched from ammonium limitation to oxygen limitation (see Fig. 1). During phase III intentional disturbances in the residual ammonium concentration were targeted (see section 3.2 for further explanations about short term effects). Therefore no steady state was achieved. Nitrate built up at higher concentrations when residual ammonium concentration was slightly decreased, indicating a direct and fast effect between high residual ammonium and NOB repression. The fast transitions (within 24 hours) cannot be explained by a community shift.

At day 141, due to increasing biomass activity, the inflow rate needed to maintain a certain ammonium effluent concentration had increased to levels that gave practical problems. Therefore, roughly half of the biomass was removed from the reactor to be able to operate at lower inflow rates again (Fig. 1A). After day 151 the airflow rate was increased from 4.2 to 6.6 L/h. The DO concentration was increased to enhance the activity of AOB to better develop the AOB layer on the granule surface and completely outcompete NOB from the granule surface. At day 168 the inflow rate was lowered again to ca. 10 L/d to decrease the residual ammonium concentration.

Phase IV

During phase IV (day 169-186) an average bulk ammonium concentration of ca. 2 mg N/L was reached (Table 1). NOB activity increased rapidly and effluent nitrate concentration increased to ca. 36 mg N/L (day 186). This was indicating that an ammonium concentration of ca. 2 mg N/L was not high enough to repress NOB effectively, even under oxygen

limitation. During days 175 to 182 a pseudo-steady state was reached with concentrations of 1.8 ± 0.1 mg $N\text{-}NH_4^+$/L, 27 ± 6 mg $N\text{-}NO_2^-$/L, 21 ± 7 mg $N\text{-}NO_3^-$/L and 3.6 ± 0.2 mg O_2/L. Also during phase IV, the specific biomass activity had increased by more than the double compared to the specific biomass activity before the removal (Table 1).

At day 173 it was noted that the effluent tube, from which samples were withdrawn, contained biofilm which contributed to the measured concentrations of ammonium, nitrite and nitrate. Comparison of a sample after the effluent tube and a sample directly from the reactor provided the insight that during the previous measurements, in general the ammonium and nitrite concentration were underestimated (measured errors of ca. 3 mg $N\text{-}NH_4^+$/L and 3 mg $N\text{-}NO_2^-$/L) and the nitrate concentrations were overestimated (measured error of ca. 7 mg $N\text{-}NO_3^-$/L), indicating that the NOB repression was effective in the reactor, but not in the tube-biofilm. From day 173 onwards samples used for the water quality measurements were withdrawn directly from the top section of the reactor. The measured errors were evaluated once the biofilm grown on the tube developed for more than 4 weeks, providing the maximum possible bias. In earlier stages of biofilm development on the inner tube wall, a more reduce impact on the results presented is expected.

Phase V

At day 187 (start of phase V, phase V: days 187-223) the bulk ammonium concentration was increased from ca. 2 to ca. 25 mg N/L. The change in the residual ammonium concentration resulted in a very fast NOB repression, and effluent nitrate concentration rapidly decreased. After a week of operation the DO was decreased by lowering the airflow rate from 6.6 to 4.2 L/h to repress even more the NOB activity. A slight decrease in the nitrate concentration during this phase was observed. A pseudo-steady state was obtained (days 193-214), 27.2 ± 0.8 mg $N\text{-}NH_4^+$/L, 17.1 ± 1.6 mg $N\text{-}NO_2^-$/L, 4.9 ± 1.3 mg $N\text{-}NO_3^-$/L and 2.7 ± 0.5 mg O_2/L.

3.2 Short-term effects of the residual ammonium concentration

Especially during phases II and III of the continuous operation, the residual ammonium concentration influenced the nitrate build-up (Fig. 1E). With increasing and decreasing ammonium concentrations, a fast (inverse) response was measured for nitrate concentrations. The corresponding change in the nitrate concentration resulted from the change in the ammonium oxidation rate of AOB (Table S2). Higher specific ammonium oxidation rates were observed when residual ammonium concentration was increased, which contributed to a lower DO concentration (Table S2). In parallel with the short term increase on the specific ammonium oxidation rate, a decrease in specific nitrate production rate was measured (Table S2). The change in the bulk ammonium concentrations impacts the nitrate concentration immediately, in a period of hours. This fast response is a clear indication that the residual ammonium concentration can be used as controlled variable for nitritation as pointed out previously (Jemaat et al., 2013).

Additionally, to present in a more direct way the short term effects of residual ammonium concentration on NOB repression, all data from day 50 onwards has been plotted in Fig. 2A. There is a clear trend in Fig. 2A, showing how NOB repression is achieved at ammonium concentrations higher than ca. 5 mg N/L, regardless to the DO concentration applied, which overall was in a wide range, from 0.7-3.7 mg O_2/L. When the time between measurements was less than 1 day, the corresponding data were highlighted in Fig. 2. For those points the sample was withdrawn 2.5 hours after the previous measurement, which is in the order of magnitude of the hydraulic retention time, therefore too short to washout the nitrate accumulated at low residual ammonium even if NOB repression is effective.

For comparison, a similar graph was plotted by including the bulk DO/ammonium concentrations ratio in the bulk liquid in Fig. 2B. In the inset graph in Fig. 2B a zoomed in

version of the graph is also given. The correlation between the bulk DO/ammonium concentrations ratio and NOB repression is less evident (compared to Fig. 2A), mainly due to the scale and the effect of the ratio itself, which produces small values at high bulk ammonium concentrations. For values of the ratio lower than 1, NOB repression is more effective (Fig. 2B, inset graph).

Batch test

A batch-test was performed at day 159 (Fig. 3) to further investigate the residual ammonium concentrations range causing the switch from effective NOB repression to nitrate production. An ammonium pulse was added after the inflow rate was stopped (time zero in Fig. 3). For bulk ammonium concentrations in the range 2-4 mg N/L the nitrate concentration increased at a higher rate (in accordance with the continuous operation results in Fig. 3), indicating the ammonium concentration causing the switch between effective NOB repression and nitrification was occurring.

The oxygen consumption rate increased ca. 8% immediately after the ammonium pulse. Interestingly, when at t= 45min the bulk ammonium concentration is back to the initial 10 mg N/L, the DO concentration is still well below the initial value, as indicated in Fig. 3 by ΔDO. This increased oxygen consumption rate at the same bulk ammonium concentration (10 mg N/L) happens despite the pH (which is not controlled) decreased by ca. 0.2.

Step-up increase in residual ammonium concentration

The step-up disturbance in the bulk ammonium concentration at day 187 produced a decrease in the DO concentration due to the increase in specific ammonium oxidation rate (Fig. 4A). As a result, the nitrate concentration rapidly decreased (Fig. 4A). The stabilization of the

ammonium oxidation rate occurred several days after the step-up disturbance, with higher rates measured immediately after the disturbance (Fig, 4A). Interesting to emphasize that the DO concentration decreased only during the transient state (3 days). Hydroxylamine at steady state conditions was not detected throughout the operation period. However, the increase in residual ammonium concentration after the step-up disturbance, resulted in hydroxylamine released into the bulk liquid, achieving a maximum value of 0.056 mg N-NH_2OH/L after 7 hours (Fig. 4C). However the monitoring of the hydroxylamine was not continued until the next morning, when hydroxylamine was not detected anymore. In addition, an increase in N_2O emission was also measured in the off-gas (Fig. 4B). No significant nitric oxide (NO) emission was observed. During the stabilisation of the residual ammonium concentration the N_2O emissions decreased again.

3.3 Biomass characteristics and sludge retention time

The biomass concentration in the reactor was plotted in Fig. 1A. The average diameter of the granules was 0.9, 1.4 and 1.3 mm, at days 0, 47 and 123 respectively (Table S2). Due to the wide size distribution, the full size distribution curve was presented in the supplementary information (Figs. S2-S4). Sludge retention time was 75 days at day 55 of continuous operation. From day 118 onwards stabilized at ca. 210±18 days. An average solids concentrations mass ratio of 0.91 gVSS/gTSS was determined. A clear colour change of the biomass over time was noticeable (Figs. S5-S7). At the day of inoculation the granules had a dark (brownish) colour, indicating the presence of heterotrophic bacteria near the granule surface and not stratification of an AOB layer. Over time the granules became orange coloured indicating the presence of active AOB bacteria in the outermost layer of the granules.

3.4 Fluorescence In Situ Hybridization (FISH)

Cryosectioned samples of the granular sludge were used for FISH analysis. Granules from day 148 and 223 were obtained from periods at high residual ammonium concentration, whereas those at day 187 were from a period at low residual ammonium concentration (see Fig. 1E). The granule structure from the three samples was highly similar (Fig. 5), presenting a clear stratification: a shell consisting of AOB colonies and behind it, the majority of the NOB colonies. The size of AOB and NOB microcolonies was difficult to measure on the pictures, because individual colonies were difficult to distinguish in both layers, but in particular in the AOB shell. Comparing the granule structure obtained in this study (Fig. 5) to the original inoculum (Fig. S8), the degree of stratification was enhanced during the operation of the reactor.

Regarding the predominant NOB species in the granular sludge, at day 148 only *Nitrospira* spp. were detected (Fig. S9) (but not *Nitrobacter* spp.). However, at day 223 both *Nitrospira* spp. and *Nitrobacter* spp. were detected (Fig. S10). *Nitrobacter* spp. were found in lower amounts than *Nitrospira* spp., indicating the development of this population during the reactor operation.

Although the quantification of the relative abundances of AOB and NOB in the granular sludge was not specifically targeted, a healthy NOB population was retained in the granular sludge during the whole period of operation, since a very fast and significant nitrate production was noticeable as soon as the imposed conditions did not efficiently repress NOB.

3.5 pH gradient in the granule and apparent ammonium half-saturation coefficient

The gradient of pH in the granule was assessed by measuring the pH difference between the core of the granule and the bulk liquid, for a pH range of 7.0-8.4 (a complete pH profile in a granule is also presented as an example, see Fig. S11). Granules were withdrawn from the reactor during phase V. The ammonium consumption in the measuring chamber was negligible. For the entire investigated range of bulk pH, a lower pH was measured inside the granule (Fig. 6). The pH curves in Fig. 6 show that at a pH in the bulk of 7.7, which is the pH inside the reactor during continuous operation, the pH difference between the bulk liquid and inside the granule was 0.44 for both ammonium concentrations tested (11 and 49 mg N/L).

A rough estimation of the AOB apparent half-saturation coefficient for ammonium ($K_{S,NH4+}^{App}$) was obtained by using a ratio of average specific ammonium oxidation rates (Eq. 3). These AOB rates 17.3±0.4 mg N-NH_4^+/(g VSS·h) from days 158–165 with an average ammonium concentration of 9 mg N-NH_4^+/L ($r_{AOB}^{9mgN/L}$), and 11.2±0.2 mg N-NH_4^+/gVSS/h from days 175-187 with an average ammonium concentration of 2 mg N/L ($r_{AOB}^{2mgN/L}$)) were obtained from periods with different ammonium concentrations, but with similar bulk DO concentrations, in order to simplify for the oxygen Monod term (see Eq. 1). Solving Eq. 3 resulted in a $K_{S,NH4+}^{App}$ of 1.7 mg N-NH_4^+/L.

$$\frac{r_{AOB}^{2mgN/L}}{r_{AOB}^{9mgN/L}} \approx \frac{\frac{2}{\left(K_{S,NH4+}^{App}+2\right)}}{\frac{9}{\left(K_{S,NH4+}^{App}+9\right)}} \quad (3)$$

3.6 Anammox

Within a couple of weeks after inoculation, Anammox activity in the reactor was lost. Until day 12 during the start-up of the reactor, Anammox activity increased as can be seen from the nitrogen balance (Fig. 1D). From day 12 onwards, the activity decreased.

At day 48 an anoxic batch-test was performed (see results in Fig. S12). During the test no clear signs of Anammox activity were detected. The decrease in ammonium, nitrite and nitrate concentrations are possibly linked to salt precipitation (for instance struvite). Ammonia stripping could also have contributed to decrease the ammonium concentration in time. FISH results from day 167 of the operation also showed a significant amount of dead cell material (no hybridization with EUB338), whereas FISH results from the last day of operation confirmed the decay of Anammox (no hybridization with AMX820) (Fig. S13).

4. Discussion

4.1 Nitritation and NOB repression

The control of the residual ammonium concentration confirmed its effectiveness on NOB repression at 20°C and pH 7.6-7.8. Stable nitritation was maintained above bulk ammonium concentrations of ca. 5 mg N/L and nitrate production was enhanced at a residual ammonium concentration of ca. 2 mg N/L (Fig. 2A).

In the conditions tested, rather than the DO/ammonium concentrations ratio (Fig. 2B), the ammonium concentration was the main factor regulating NOB repression (Fig. 2A). The DO/ammonium concentrations ratio required for efficient NOB repression was ca. 1 mg O_2/mg N or lower (Fig. 2B). Bartrolí et al., 2010 operating at 30ºC found that the required value of the ratio was ca. 0.18 mg O_2/mg N or lower. Reasons for this difference remain until now unclear. We hypothesize that the difference in behavior comes from the difference in granule structure. In our study, the inoculum was a granular sludge containing anammox in the granule core (Fig. 5). However, in Bartrolí et al. (2010), or in similar trials using the DO/ammonium concentration ratio as main criterion, the granular sludge did not contain anammox.

The production of nitrate in the biofilm grown on the effluent tube inner wall is probably due to the diffusion of oxygen through the tube wall (that type of silicone tube is permeable to oxygen). The counter-diffusion of oxygen makes oxygen available to NOB and stratification is useless to keep nitritation stable.

4.2 Stratification of AOB and NOB populations

Stratification of AOB and NOB populations in granular sludge has been sometimes reported when removing nitrogen through one stage partial nitritation / anammox (Vlaeminck et al., 2010; Winkler et al., 2011). In such systems, anammox bacteria are located in the core of the granule and act as a sink for nitrite, facilitating NOB repression and perhaps stratification. Nevertheless, for nitrifying granules, to the best of our knowledge, only one study reported stratification of AOB and NOB in granular sludge reactor (Tsuneda et al., 2003). Their granular sludge was cultivated in an aerobic upflow fluidized bed treating high strength ammonium wastewater. The reasons why the stratification developed and the significance of their findings were not discussed, not even in subsequent reports when mathematical modelling was used to describe the experimental findings (Matsumoto et al., 2010). In fact both mathematical models used (one and two dimensional biofilm models) failed to describe the stratification (Matsumoto et al., 2010). In this study, we found stratification of AOB and NOB for the first time when treating low strength wastewater and operating at 20ºC. There are two aspects associated to the stratified structure: (i) the position of the AOB microcolonies is better for oxygen competition because they are much closer to the granule surface, enhancing NOB repression; (ii) the outer dense AOB shell acts as a protective layer for NOB microcolonies against detachment, delaying washout of NOB from the granular sludge.

In such stratified granule, the oxygen penetration depth could therefore play a clear role in NOB repression. When AOB preferentially occupy the external shell of the granule, the competition for oxygen between AOB and NOB is deeply impacted, as demonstrated through a 3-dimensional modelling study in which the effect of the presence of cell clusters was specifically targeted (Picioreanu et al., *submitted*).

Secondly, the NOB colonies occupying inner layers are protected against detachment. Their residence time in the reactor is expected to be longer than that of AOB. Moreover, a larger cluster size (compared to that of AOB microcolonies) could be achieved in time. In general, larger NOB colonies behind the AOB layer would be easier to repress due to smaller surface to volume ratios. However, due to the intensity of the signal, it is not possible to estimate a representative average size for AOB and NOB cell clusters, and therefore this hypothesis could not be proven at this stage.

In this type of granular sludge, NOB is known to persist for long periods of time (several months), despite nitrate production was measured to be at very low levels (Bartrolí et al., 2010; Lotti et al., 2014b; Isanta et al., 2015, among others). In our study, also the same trend is observed. This would indicate an alternative metabolic NOB route to survive in absence of oxygen. The ability of some NOB to reverse their main oxidative reaction (i.e. to reduce nitrate into nitrite) has been reported, when there is absence of oxygen but availability of COD (e.g. formate) (Koch et al., 2015). In this case, where an autotrophic synthetic medium is used, this possibility might be only plausible if NOB could use the organic matter formed from decay products. Additionally, complete ammonium oxidation (comammox) *Nitrospira* were found at high abundances in an autotrophic culture in anoxic conditions, although their primary metabolic route remained unknown (van Kessel et al., 2016).

Some NOB colonies were located closer to the granule surface, surrounded by AOB colonies (Fig. 5). These NOB colonies were assumed to be the reason for the residual nitrate concentration in the reactor.

Previous studies reported the presence of *Nitrobacter* spp. as the dominant NOB species when controlling the residual ammonium to repress NOB and hypothesized that a prerequisite to obtain stable partial nitritation could be to select *Nitrobacter* spp. instead of *Nitrospira* spp. (Isanta et al., 2015). Wang et al. (2016) reported that the strategy of controlling residual ammonium at high concentrations would only be successful in the case of *Nitrobacter* spp. (r-strategist) being the dominant NOB population. However, here we found that a high residual ammonium concentration enhanced AOB stratification in the external granule layer, which demonstrated to be a successful strategy independently of the initial NOB genus found in the sludge.

4.3 Linking the effects of the DO/ammonium concentrations ratio to stratification

Higher residual ammonium concentrations result in higher ammonium oxidation rates (Table 1, Fig. 4A, Table S2) which in turn would allow to apply higher DO concentrations in a reactor without compromising the stability of nitritation (in agreement with Bartrolí et al., 2010). Simply because the oxygen penetration depth is shorter at higher ammonium oxidation rates. This is therefore the fundamental mechanism explaining the correlation found between the bulk DO/ammonium concentrations ratio and NOB repression in Bartrolí et al. (2010). In that study, at 30ºC, NOB repression was achieved at residual ammonium concentration of 40 mg N/L and DO = 7 mg O_2/L (DO/ammonium= 0.18 g O_2/g N) and for 20 mg N/L and DO = 5 mg O_2/L (DO/ammonium= 0.25 g O_2/g N), but complete nitrification at residual ammonium concentration of 20 mg N/L and DO = 7 mg O_2/L (DO/ammonium= 0.35 g O_2/g N).

To effectively repress NOB in wastewater treatment systems containing granular sludge, stratification of AOB and NOB inside the granule structure is identified here as a requirement. Without the stratification, NOB colonies can grow closer towards the granule surface where they have better access to oxygen resulting in nitrate production. This is in agreement with the assessment of oxygen competition through 3-D modelling of granules containing cell clusters (Picioreanu et al., *submitted*). A complete and dense AOB layer on the granule surface would result in a limited oxygen penetration depth, and no oxygen available for the inner layers where NOB are located. Stratification of AOB on the granule surface can be created by operating at high residual ammonium concentrations, to enhance high ammonium oxidation rates.

By applying high residual ammonium concentrations, AOB consume most of the oxygen resulting in the repression of NOB. When in time the nitrate production becomes low enough, indicating good stratification, the possibility arises to decrease the residual ammonium concentration. However, the residual ammonium concentration has its lower limits for successful NOB repression, as reported in this study. Maintaining a high residual ammonium concentration would not be preferred in all autotrophic nitrogen removal systems. The strategy would be suited for a two stage nitrogen removal process, where in the first stage partial nitritation is desired (so in combination with Anammox in a second stage). In this system the residual ammonium concentration has to be high, due to design requirements, since only 50% of the ammonium has to be oxidised to nitrite in order to supply Anammox with the right distribution in N substrates. However, this strategy would not be suited for single stage autotrophic nitrogen removal, as high residual ammonium concentrations in this system are not desired, since the aim is the removal of nitrogen from the wastewater. Plug-flow hydrodynamics or SBR operation could be used instead in one-stage nitrogen removal systems, to enhance the use of high residual ammonium concentrations as previously

499 highlighted in the literature (Pérez et al., 2014). For full scale applications, diurnal variability
500 of the wastewater, seasonality and rainy events might be also hampering the control of the
501 residual ammonium concentration in the partial nitritation reactor (Pérez et al., 2015). The use
502 of reject water might assist to overcome (some of) these issues, as already assessed by
503 mathematical modelling (Pérez et al., 2015).

504

505 **4.4 pH gradient in the granule**

506 Because ammonia is reported to be the true substrate for AOB (Suzuki et al., 1974), the lower
507 pH inside the granule leads to a lower ammonia concentration in the inner parts due to the
508 ammonium-ammonia acid-base equilibrium. The pH difference between bulk liquid and
509 granule core ($\Delta pH = 0.44$ see Fig. 6) was in the same range found for similar systems (de
510 Beer et al., 1993; Gieseke et al., 2006; Schreiber et al., 2009; Uemura et al., 2011; Winkler et
511 al., 2011) or calculated through mathematical models (Park et al., 2010). Since an increase in
512 the bulk ammonium concentration results in higher ammonium oxidation rates, the pH
513 towards the centre of the granule would decrease even further due to the increase in proton
514 production by AOB. Therefore, higher residual ammonium concentrations lead to an even
515 higher $K_{S,NH4+}$ value towards the centre of the granule due to the larger decrease in pH in
516 these regions, making these inner located cells even less saturated in ammonia. This creates
517 the possibility of further increases in the residual ammonium concentration to obtain higher
518 ammonium oxidation rates, resulting in both enhancement of the stratification and in NOB
519 repression. The limitation of the enhancement of the rate is that at pH too distant from the
520 optimal pH range of AOB, the maximum specific ammonium oxidation rate would
521 significantly decrease.

Suzuki et al. (1974) measured how the ammonium half-saturation coefficient ($K_{S,NH4+,}$ expressed in units of nitrogen ammonium) changes with pH. The lower pH leads to a higher $K_{S,NH4+}$ value inside the granule. With use of the measured pH gradient, the pH effect on the ammonium half-saturation coefficient for AOB ($K_{S,NH4+}$(pH)) was assessed (see Eqs. S1-S2 in the supplementary information, section S2.8) (Table 2).

The apparent ammonium half-saturation coefficient would increase by a factor of 2.7 times with a decrease in pH of 0.44 (Table 2), indicating that AOB cells exposed to a lower pH (those located further away from the granule surface) could be less saturated in ammonium than those at the granule surface. Therefore, these cells would have an advantage when the bulk ammonium concentration is increased (see the corresponding change in the ammonium Monod term in Table 2).

However, the pH also affects the maximum specific growth rate of AOB (μ_{max}^{AOB}). To assess the overall impact of pH on the ammonium oxidation rate, the influence on both μ_{max}^{AOB} and $K_{S,NH4+}$ was taken into account as shown in Table 2. Values were used to assess qualitatively how the pH gradient could explain the increase in oxygen consumption detected in the batch test presented in Fig. 3. Comparing only the ammonium Monod term at the pH of the granule core for ammonium concentrations of 10 and 20 mg N/L, there is a clear advantage (16% increase). Nevertheless, the μ_{max}^{AOB} value is also smaller at the lower pH (with a decrease of ca. -15%, between pH of the bulk and pH of the granule core, see Table 2), which would decrease the overall contribution to the observed ammonium oxidation rate. Also for the batch test conditions, the bulk DO decreased from 3.1 to 2.6 mg O_2/L, which should also penalize the ammonium oxidation rate through the oxygen Monod term (see Eq. 1), even more for cells in the inner layers, at a lower pH. Additionally, the pH decreased just after the pulse. Interestingly, despite the negative effects (decrease in DO and pH), the oxygen consumption rate increased.

When the microsensor is used into the granule for measuring the pH, it is unlikely that the microcolonies (i.e. the dense cell clusters in which AOB and NOB grow in the biofilm) are perforated, due to the strong adhesion properties of the EPS in the microcolony (Larsen et al., 2008). The microsensor tip probably would push away those colonies. The pH profile inside the microcolony is therefore expected to be even steeper than that measured in the biofilm matrix, because of the high density in the cell cluster (ca. 600 gCOD/L, Coskuner et al., 2005). Therefore, although the pH gradients are here discussed as being one dimensional along the biofilm depth, they would also develop inside the colonies. This applies not only for pH, but also for oxygen and substrate.

Overall, a truly quantitative impact of the pH gradient on AOB activity is at this stage not conclusive. It would require of three-dimensional biofilm modelling, including the description of the cell clusters. The model might help to clarify if the pH gradient would explain the higher measured oxygen consumption and the higher ammonium oxidizing rates when residual ammonium concentrations are increased.

4.5 Ammonia gradient in the granule

The ammonia gradient in the granule is influenced by both diffusion and the pH gradient. Through diffusion the ammonium concentration tends to decrease in the inner layers of the granules (i.e. ammonia is consumed by AOB, and overall the total ammoniacal nitrogen is therefore decreasing). However, the expected decrease would be rather low, because oxygen is stoichiometrically limiting. Additionally, the pH decreases in the inner layers of the granule due to the protons produced by AOB. Therefore at a lower pH the fraction of free ammonia is even lower. The effect of the pH dominates the gradient of ammonia. To numerically clarify the contributions, we used as example the following conditions: DO = 3.5 mg O_2/L and temperature 20ºC. Assuming a concentration of 20 mg N/L and pH 7.7 in bulk liquid, the free ammonia concentration is 0.67 mg N/L (see Table S3). Since the oxygen is limiting and the

572 stoichiometry of the nitritation makes that 3.43 g O_2/g N-NH_4^+ are required for the oxidation
573 of ammonium to nitrite. Using this factor, with the assumed DO (3.5 mg O2/L), the decrease
574 in ammonium would be ca. 1 mg N/L. Therefore the gradient of ammonia coming from the
575 decrease due to consumption by AOB (i.e. diffusion limitation) would be only 0.02 mg N-
576 NH_3/L. Assuming a decrease in the pH from 7.7 to 7.26, the decrease in ammonia would be of
577 0.3 mg N-NH_3/L, being therefore 15 times larger than the gradient due to diffusion limitation.
578 Even considering oxygen saturation, the decrease in ammonium would be from 20 to 17.7,
579 which would mean a decrease in ammonia of 0.05, still three times lower than the effect of
580 pH. In conclusion, the gradient of ammonia is dominated by the pH gradient, rather than due
581 to diffusion limitation (due to ammonia consumption by AOB). However, both effects
582 contribute and decrease the ammonia towards the inner layers of the granule.

583 **4.6 Implications of hydroxylamine release after a step-up increase in residual**
584 **ammonium concentration**

585 Hydroxylamine has been reported to be able to increase the AOB growth rate, in case of the
586 mixotrophic growth of AOB on ammonia and hydroxylamine under substrate-limited growth
587 conditions (De Bruijn et al., 1995; Harper et al., 2009). Hydroxylamine produced an increase
588 in the ammonia uptake rate of AOB in the short term (De Bruijn et al., 1995). In addition,
589 hydroxylamine has been reported to be highly inhibitory for NOB (Yang and Alleman, 1992;
590 Blackburne et al., 2004; Noophan et al., 2004). Both effects of hydroxylamine could in theory
591 support the repression of NOB, when increasing the residual ammonium concentration from
592 low concentrations to a high residual ammonium concentration. The hydroxylamine that is
593 temporarily accumulated (as reported in this study), could enhance the growth rate of AOB
594 and simultaneously inhibit NOB.

595 The strong gradients of oxygen and pH that develop in the dense AOB cell clusters might
596 create different niches, in which hydroxylamine released by ammonia saturated cells might be

cometabolized by other AOB cells, that are more interior in the AOB layer, or in the cell cluster. This cometabolization would require of cells that have oxygen availability, but still are not suffering ammonium saturation. This is plausible given the pH gradient found, where the ammonium saturation condition depends on the pH, as already discussed. In addition, studies of the kinetics and pH-dependency of ammonia and hydroxylamine oxidation by *Nitrosomonas europaea* revealed that hydroxylamine oxidation is moderately pH-sensitive, whereas ammonia oxidation decreases strongly with decreasing pH (Frijlink et al., 1992). Which would support that, the steep pH gradients produce a pool of ammonia non-saturated cells that use hydroxylamine in aerobic environments without being much affected by the low pH values attained. This hypothesis would therefore provide a new mechanism for the positive effects of applying high residual ammonium concentrations for NOB repression. This could be linked with the transient effects of the increase in residual ammonium concentration as highlighted in the short term effects (Fig. 3 and 4). Particularly interesting is the large increase in the specific ammonium oxidation rate (from 11 to 21mg N/(g VSS·h), Fig. 4) during the first hours after the increase in ammonium (Fig. 4). The specific ammonium oxidation rate was calculated also based on the nitrite and nitrate production (summing up both, Fig. 4A), to rule out any potential absorption process in the granular sludge, since ammonium absorption in granular sludge is known to happen (Bassin et al., 2011). However, further research is required to be able to obtain conclusive evidence about the effects of the hydroxylamine release on the ammonium oxidation rate.

Hydroxylamine diffusing to deeper layers (either in the granule or in the AOB cell cluster) where there is no oxygen availability triggers nitrifier denitrification, since nitrite is also present, as suggested previously for biofilms in a theoretical model based study (Sabba et al., 2015). Therefore the simultaneous detection of hydroxylamine and a significant increase in N_2O emissions, could be associated to the nitrifier denitrification pathway.

NOB inhibited by hydroxylamine produced by AOB would not be a very plausible explanation, because the levels detected in this study are very low as to be inhibitory (Blackburne et al., 2004; Noophan et al., 2004). In addition, for long term exposure to the inhibitory compound, acclimation of the bacteria would be expected.

5. Conclusions

- The control of the residual ammonium concentration has proven to be effective for repression of *Nitrospira* spp. at 20°C. The switch in NOB repression to NOB proliferation was determined to be located in a bulk ammonium concentration range of 2-5 mg N/L for DO concentrations lower than 4 mg O_2/L.
- Operating at higher residual ammonium concentration triggers higher ammonium oxidation rates and higher oxygen consumption rates, both in the short and long term.
- Stratification of an outer AOB layer in the granule structure was found to be highly important to maintain stable partial nitritation in the long term. The AOB layer is important to achieve oxygen limitation for NOB due to the oxygen penetration depth in combination with bulk ammonium concentrations which are high enough to prevent rate-limiting conditions for AOB.
- The pH gradient found provides an explanation for the direct effect of residual ammonium in the ammonium oxidation rate, because cells located further away from the granule surface are less saturated in ammonia due to the decrease in pH. This contributes to NOB repression.

Acknowledgements

JP work was supported a Marie Curie Intra European Fellowship (GreenN2, PIEF-GA-2012-326705). This research was funded by the SIAM Gravitation Grant 024.002.002, the Netherlands Organization for Scientific Research.

References

Abma, W.R., Driessen, W., Haarhuis, R., Van Loosdrecht, M.C.M., 2010. Upgrading of sewage treatment plant by sustainable and cost-effective separate treatment of industrial wastewater. Water Sci. Technol. 61, 1715–1722. doi:10.2166/wst.2010.977

APHA, 2012. Standard Methods for the Examination of Water and Wastewater, American Water Works Association/American Public Works Association/Water Environment Federation.

Bartrolí, A., Pérez, J., Carrera, J., 2010. Applying ratio control in a continuous granular reactor to achieve full nitritation under stable operating conditions. Environ. Sci. Technol. 44, 8930–8935. doi:10.1021/es1019405

Bassin, J.P., Pronk, M., Kraan, R., Kleerebezem, R., Van Loosdrecht, M.C.M., 2011. Ammonium adsorption in aerobic granular sludge, activated sludge and anammox granules. Water Res. 45, 5257–5265. doi:10.1016/j.watres.2011.07.034

Blackburne, R., Carvalho, G., Yuan, Z., Keller, J., 2004. Selective Production of Nitrite Using Hydroxylamine As Inhibitor of Nitrite Oxidation. Water Environ. Manag. Ser. 189–196.

Blackburne, R., Yuan, Z., Keller, J., 2008. Partial nitrification to nitrite using low dissolved oxygen concentration as the main selection factor. Biodegradation 19, 303–312. doi:10.1007/s10532-007-9136-4

Bougard, D., Bernet, N., Chèneby, D., Delgenès, J.P., 2006. Nitrification of a high-strength wastewater in an inverse turbulent bed reactor: Effect of temperature on nitrite

accumulation. Process Biochem. 41, 106–113. doi:10.1016/j.procbio.2005.03.064

Brockmann, D., Morgenroth, E., 2010. Evaluating operating conditions for outcompeting nitrite oxidizers and maintaining partial nitrification in biofilm systems using biofilm modeling and Monte Carlo filtering. Water Res. 44, 1995–2009. doi:10.1016/j.watres.2009.12.010

Coskuner, G., Ballinger, S.J., Davenport, R.J., Pickering, R.L., Solera, R., Head, I.M., Curtis, T.P., 2005. Agreement between Theory and Measurement in Quantification of Ammonia-Oxidizing Bacteria. Appl. Environ. Microbiol. 71, 6325–6334. doi:10.1128/AEM.71.10.6325

de Beer, D., Heuvel, J.C. van den, Ottengraf, S.P.P., 1993. Microelectrode measurement of the activity distribution in nitrofying bacterial aggregates. Appl. Environ. Microbiol. 59, 573–579.

De Bruijn, P., van de Graaf, A.A., Jetten, M., Robertson, L., Kuenen, J., 1995. Growth of Nitrosonomas europaea on hydroxylamine. FEMS Microbiol Lett 125, 179–84.

De Clippeleir, H., Vlaeminck, S.E., De Wilde, F., Daeninck, K., Mosquera, M., Boeckx, P., Verstraete, W., Boon, N., 2013. One-stage partial nitritation/anammox at 15 C on pretreated sewage: Feasibility demonstration at lab-scale. Appl. Microbiol. Biotechnol. 97, 10199–10210. doi:10.1007/s00253-013-4744-x

Frear, D.S., Burrell, R.C., 1955. Spectrophotometric Method for Determining Hydroxylamine Reductase Activity in Higher Plants. Anal. Chem. 27, 1664–1665. doi:10.1021/ac60106a054

Frijlink, M.J., Abee, T., Laanbroek, H.J., de Boer, W., Konings, W.N., 1992. The bioenergetics of ammonia and hydroxylamine oxidation in Nitrosomonas europaea at acid and alkaline pH. Arch. Microbiol. 157, 194–199. doi:10.1007/BF00245290

Fux, C., Siegrist, H., 2003. Nitrogen removal from sludge digester liquids by nitrification /

695 denitrification or partial nitritation / anammox : environmental and economical
696 considerations 19–26.
697 Garrido, J.M., Van Benthum, W.A.J., Van Loosdrecht, M.C.M., Heijnen, J.J., 1997. Influence
698 of dissolved oxygen concentration on nitrite accumulation in a biofilm airlift suspension
699 reactor. Biotechnol. Bioeng. 53, 168–178. doi:10.1002/(SICI)1097-
700 0290(19970120)53:2<168::AID-BIT6>3.0.CO;2-M
701 Gieseke, A., Tarre, S., Green, M., De Beer, D., 2006. Nitrification in a biofilm at low pH
702 values: Role of in situ microenvironments and acid tolerance. Appl. Environ. Microbiol.
703 72, 4283–4292. doi:10.1128/AEM.00241-06
704 Gilbert, E.M., Agrawal, S., Karst, S.M., Horn, H., Nielsen, P.H., Lackner, S., 2014. Low
705 temperature partial nitritation/anammox in a moving bed biofilm reactor treating low
706 strength wastewater. Environ. Sci. Technol. 48, 8784–8792. doi:10.1021/es501649m
707 Guisasola, A., Jubany, I., Baeza, J.A., Carrera, J., Lafuente, J., 2005. Respirometric
708 estimation of the oxygen affinity constants for biological ammonium and nitrite
709 oxidation. J. Chem. Technol. Biotechnol. 80, 388–396. doi:10.1002/jctb.1202
710 Han, M., De Clippeleir, H., Al-Omari, A., Wett, B., Vlaeminck, S.E., Bott, C., Murthy, S.,
711 2016. Impact of carbon to nitrogen ratio and aeration regime on mainstream
712 deammonification. Water Sci. Technol. 1–11. doi:10.2166/wst.2016.202
713 Harper, W.F., Terada, A., Poly, F., Le Roux, X., Kristensen, K., Mazher, M., Smets, B.F.,
714 2009. The effect of hydroxylamine on the activity and aggregate structure of autotrophic
715 nitrifying bioreactor cultures. Biotechnol. Bioeng. 102, 714–724. doi:10.1002/bit.22121
716 Harremoes, P., 1982. Criteria for nitrification in fixed film reactors. Water Sci. Technol. 14,
717 167–187.
718 Hellinga, C., Schellen, A.A.J.C., Mulder, J.W., Van Loosdrecht, M.C.M., Heijnen, J.J., 1998.
719 The SHARON process: An innovative method for nitrogen removal from ammonium-

720 rich waste water. Water Sci. Technol. 37, 135–142. doi:10.1016/S0273-1223(98)00281-
721 9
722 Hunik, J.H., Bos, C.G., Van den Hoogen, M.P., De Gooijer, C.D., Tramper, J., 1994. Co-
723 immobilized Nitrosomonas europaea and Nitrobacter agilis cells: Validation of a
724 dynamic model for simultaneous substrate conversion and growth in κ-carrageenan gel
725 beads. Biotechnol. Bioeng. 43, 1153–1163. doi:10.1002/bit.260431121
726 Isanta, E., Reino, C., Carrera, J., Pérez, J., 2015. Stable partial nitritation for low-strength
727 wastewater at low temperature in an aerobic granular reactor. Water Res. 80, 149–158.
728 doi:10.1016/j.watres.2015.04.028
729 Jemaat, Z., Bartrolí, A., Isanta, E., Carrera, J., Suárez-Ojeda, M.E., Pérez, J., 2013. Closed-
730 loop control of ammonium concentration in nitritation: Convenient for reactor operation
731 but also for modeling. Bioresour. Technol. 128, 655–663.
732 doi:10.1016/j.biortech.2012.10.045
733 Jubany, I., Carrera, J., Lafuente, J., Baeza, J.A., 2008. Start-up of a nitrification system with
734 automatic control to treat highly concentrated ammonium wastewater: Experimental
735 results and modeling. Chem. Eng. J. 144, 407–419. doi:10.1016/j.cej.2008.02.010
736 Kartal, B., Kuenen, J.G., van Loosdrecht, M.C.M., 2010. Sewage Treatment with Anammox.
737 Science (80-.). 328, 702–703. doi:10.1126/science.1185941
738 Koch, H., Lücker, S., Albertsen, M., Kitzinger, K., Herbold, C., Spieck, E., Nielsen, P.H.,
739 Wagner, M., Daims, H., 2015. Expanded metabolic versatility of ubiquitous nitrite-
740 oxidizing bacteria from the genus Nitrospira. Proc. Natl. Acad. Sci. 112, 11371–11376.
741 doi:10.1073/pnas.1506533112
742 Larsen, P., Nielsen, J.L., Svendsen, T.C., Nielsen, P.H., 2008. Adhesion characteristics of
743 nitrifying bacteria in activated sludge. Water Res. 42, 2814–2826.
744 doi:10.1016/j.watres.2008.02.015

745 Lotti, T., Kleerebezem, R., Hu, Z., Kartal, B., de Kreuk, M.K., van Erp Taalman Kip, C.,
746 Kruit, J., Hendrickx, T.L.G., van Loosdrecht, M.C.M., 2014a. Pilot-scale evaluation of
747 anammox-based mainstream nitrogen removal from municipal wastewater. Environ.
748 Technol. 36, 1167–77. doi:10.1080/09593330.2014.982722
749 Lotti, T., Kleerebezem, R., Hu, Z., Kartal, B., Jetten, M.S.M., van Loosdrecht, M.C.M.,
750 2014b. Simultaneous partial nitritation and anammox at low temperature with granular
751 sludge. Water Res. 66, 111–121. doi:10.1016/j.watres.2014.07.047
752 Ma, B., Bao, P., Wei, Y., Zhu, G., Yuan, Z., Peng, Y., 2015. Suppressing Nitrite-oxidizing
753 Bacteria Growth to Achieve Nitrogen Removal from Domestic Wastewater via
754 Anammox Using Intermittent Aeration with Low Dissolved Oxygen. Sci. Rep. 5, 13048.
755 doi:10.1038/srep13048
756 Matsumoto, S., Katoku, M., Saeki, G., Terada, A., Aoi, Y., Tsuneda, S., Picioreanu, C., Van
757 Loosdrecht, M.C.M., 2010. Microbial community structure in autotrophic nitrifying
758 granules characterized by experimental and simulation analyses. Environ. Microbiol. 12,
759 192–206. doi:10.1111/j.1462-2920.2009.02060.x
760 Noophan, P.L., Figueroa, L.A., Munakata-Marr, J., 2004. Nitrite oxidation inhibition by
761 hydroxylamine: Experimental and model evaluation. Water Sci. Technol. 50, 295–304.
762 Park, S., Bae, W., Rittmann, B.E., Kim, S., Chung, J., 2010. Operation of suspended-growth
763 shortcut biological nitrogen removal (SSBNR) based on the minimum/maximum
764 substrate concentration. Water Res. 44, 1419–1428. doi:10.1016/j.watres.2009.11.030
765 Peng, Y., Zhu, G., 2006. Biological nitrogen removal with nitrification and denitrification via
766 nitrite pathway. Appl. Microbiol. Biotechnol. 73, 15–26. doi:10.1007/s00253-006-0534-
767 z
768 Pérez, J., Costa, E., Kreft, J.U., 2009. Conditions for partial nitrification in biofilm reactors
769 and a kinetic explanation. Biotechnol. Bioeng. 103, 282–295. doi:10.1002/bit.22249

Pérez, J., Isanta, E., Carrera, J., 2015. Would a two-stage N-removal be a suitable technology to implement at full scale the use of anammox for sewage treatment? Water Sci. Technol. 72, 858–864. doi:10.2166/wst.2015.281

Pérez, J., Lotti, T., Kleerebezem, R., Picioreanu, C., van Loosdrecht, M.C.M., 2014. Outcompeting nitrite-oxidizing bacteria in single-stage nitrogen removal in sewage treatment plants: A model-based study. Water Res. 66, 208–218. doi:10.1016/j.watres.2014.08.028

Picioreanu, C., Van Loosdrecht, M.C.M., Heijnen, J.J., 1997. Modelling the effect of oxygen concentration on nitrite accumulation in a biofilm airlift suspension reactor. Water Sci. Technol. 36, 147–156. doi:10.1002/(SICI)1097-0290(19970120)53:2<168::AID-BIT6>3.0.CO;2-M

Reino, C., Suárez-Ojeda, M.E., Pérez, J., Carrera, J., 2016. Kinetic and microbiological characterization of aerobic granules performing partial nitritation of a low-strength wastewater at 10 °C. Water Res. 101, 147–156. doi:10.1016/j.watres.2016.05.059

Sabba, F., Picioreanu, C., Pérez, J., Nerenberg, R., 2015. Hydroxylamine diffusion can enhance N2O emissions in nitrifying biofilms: A modeling study. Environ. Sci. Technol. 49, 1486–1494. doi:10.1021/es5046919

Schreiber, F., Loeffler, B., Polerecky, L., Kuypers, M.M., de Beer, D., 2009. Mechanisms of transient nitric oxide and nitrous oxide production in a complex biofilm. ISME J. 3, 1301–1313. doi:10.1038/ismej.2009.55

Sliekers, A.O., Haaijer, S.C.M., Stafsnes, M.H., Kuenen, J.G., Jetten, M.S.M., 2005. Competition and coexistence of aerobic ammonium- and nitrite-oxidizing bacteria at low oxygen concentrations. Appl. Microbiol. Biotechnol. 68, 808–817. doi:10.1007/s00253-005-1974-6

Soler-Jofra, A., Stevens, B., Hoekstra, M., Picioreanu, C., Sorokin, D., van Loosdrecht,

795 M.C.M., Pérez, J., 2016. Importance of abiotic hydroxylamine conversion on nitrous
796 oxide emissions during nitritation of reject water. Chem. Eng. J. 287, 720–726.
797 doi:10.1016/j.cej.2015.11.073
798 Suzuki, I., Dular, U., Kwok, S., 1974. Ammonia or Ammonium Ion as Substrate for
799 Oxidation by Nitrosomonas-Europaea Cells and Extracts. J. Bacteriol. 120, 556–558.
800 Third, K.A., Sliekers, A.O., Kuenen, J.G., Jetten, M.S., 2001. The CANON system
801 (Completely Autotrophic Nitrogen-removal Over Nitrite) under ammonium limitation:
802 interaction and competition between three groups of bacteria. Syst. Appl. Microbiol. 24,
803 588–596. doi:10.1078/0723-2020-00077
804 Tijhuis, L., van Loosdrecht, M.C.M., 1994. Solids retention time in heterotrophic and
805 nitrifying biofilms in a biofilm airlift suspension reactor 44, 867–879.
806 Tsuneda, S., Nagano, T., Hoshino, T., Ejiri, Y., Noda, N., Hirata, A., 2003. Characterization
807 of nitrifying granules produced in an aerobic upflow fluidized bed reactor. Water Res.
808 37, 4965–4973. doi:10.1016/j.watres.2003.08.017
809 Uemura, S., Suzuki, S., Abe, K., Ohashi, A., Harada, H., Ito, M., Imachi, H., Tokutomi, T.,
810 2011. Partial nitrification in an airlift activated sludge reactor with experimental and
811 theoretical assessments of the ph gradient inside the sponge support medium. Int. J.
812 Environ. Res. 5, 33–40.
813 Vlaeminck, S.E., Terada, A., Smets, B.F., De Clippeleir, H., Schaubroeck, T., Bolea, S.,
814 Demeestere, L., Mast, J., Boon, N., Carballa, M., Verstraete, W., 2010. Aggregate size
815 and architecture determine microbial activity balance for one-stage partial nitritation and
816 anammox. Appl. Environ. Microbiol. 76, 900–909. doi:10.1128/AEM.02337-09
817 Wang, B. Bin, Chang, Q., Peng, D.C., Hou, Y.P., Li, H.J., Pei, L.Y., 2014. A new
818 classification paradigm of extracellular polymeric substances (EPS) in activated sludge:
819 Separation and characterization of exopolymers between floc level and microcolony

level. Water Res. 64, 53–60. doi:10.1016/j.watres.2014.07.003

Wang, D., Wang, Q., Laloo, A., Xu, Y., Bond, P.L., Yuan, Z., 2016. Achieving Stable Nitritation for Mainstream Deammonification by Combining Free Nitrous Acid-Based Sludge Treatment and Oxygen Limitation. Sci. Rep. 6, 25547. doi:10.1038/srep25547

Wett, B., 2007. Development and implementation of a robust deammonification process. Water Sci. Technol. 56, 81–88. doi:10.2166/wst.2007.611

Winkler, M.K.H., Kleerebezem, R., Kuenen, J.G., Yang, J., Van Loosdrecht, M.C.M., 2011. Segregation of biomass in cyclic anaerobic/aerobic granular sludge allows the enrichment of anaerobic ammonium oxidizing bacteria at low temperatures. Environ. Sci. Technol. 45, 7330–7337. doi:10.1021/es201388t

Yang, L., Alleman, J.E., 1992. Investigation of batchwise nitrite build-up by an enriched nitrification culture. Water Sci. Technol. 26, 997–1005.

TABLES

Table 1. Characterization of the pseudo-steady states attained during reactor operation: average concentrations of N-compounds and DO, specific ammonium oxidation rate (r_{AOB}) and specific nitrate production rate (r_{NOB}). Phase III did not achieve a pseudo-state state operation; therefore, no details are given in this table but the measurements for phase III are shown in Fig. 1.

Phase	**Period**	**NH_4^+ Eff**	**NO_2^- Eff**	**NO_3^- Eff**	**Tot-N_{in}**	**Tot-N_{out}**	**DO**	**r_{AOB}**	**r_{NOB}**
	(d)	(mg N/L)	(mg N/L)	(mg N/L)	(mg N/L)	(mg N/L)	(mg O_2/L)	(mg N/(gVSS·h))	(mg N/(g VSS·h))
I	53-67	16 ± 0.9	24 ± 2	6.0 ± 1	51 ± 0.8	46 ± 0.9	0.7 ± 0.1	5.7 ± 0.6	1.0 ± 0.2
II	117-139	0.8 ± 0.3	24 ± 11	14 ± 11	43 ±4	40 ± 4	2 ± 1	5 ± 1	2 ± 2
IV	175-182	1.8 ± 0.1	27 ± 6	21 ± 7	50 ± 1	50 ± 0.7	3.6 ± 0.2	11.1 ± 0.2	5 ± 2
V	193-214	27 ± 0.8	17 ± 2	5 ± 1	51 ± 1	49.2 ± 0.4	2.7 ± 0.5	13 ± 0.9	2.7 ± 0.7

Table 2. Ammonium half-saturation coefficients for AOB at the bulk liquid pH and at the pH inside a granule at T=20°C, together with the effect of the $K_{S,NH4+}$ on the ammonium Monod term at different ammonium concentrations ($M_{NH4,i}$, where *i* is the value of ammonium concentration in mg N/L): $M_{NH4,i} = C_{S,i}/(C_{S,i}+K_{S,NH4+})$. Maximum specific growth rate (μ_{max}^{AOB}) was also calculated (at 20ºC and for the corresponding pH, as in Jubany et al., 2008) to assess the overall impact in ammonium oxidation rate.

Microelectrode position	**pH**	$K_{S,NH4+}$ **(mg N/L)**	$M_{NH4,10}$ **(dimensionless)**	$M_{NH4,20}$ **(dimensionless)**	μ_{max}^{AOB} **(1/d)**
Bulk	7.70	1.7	0.85	0.92	0.78
Granule centre	7.26	4.6	0.68	0.81	0.68

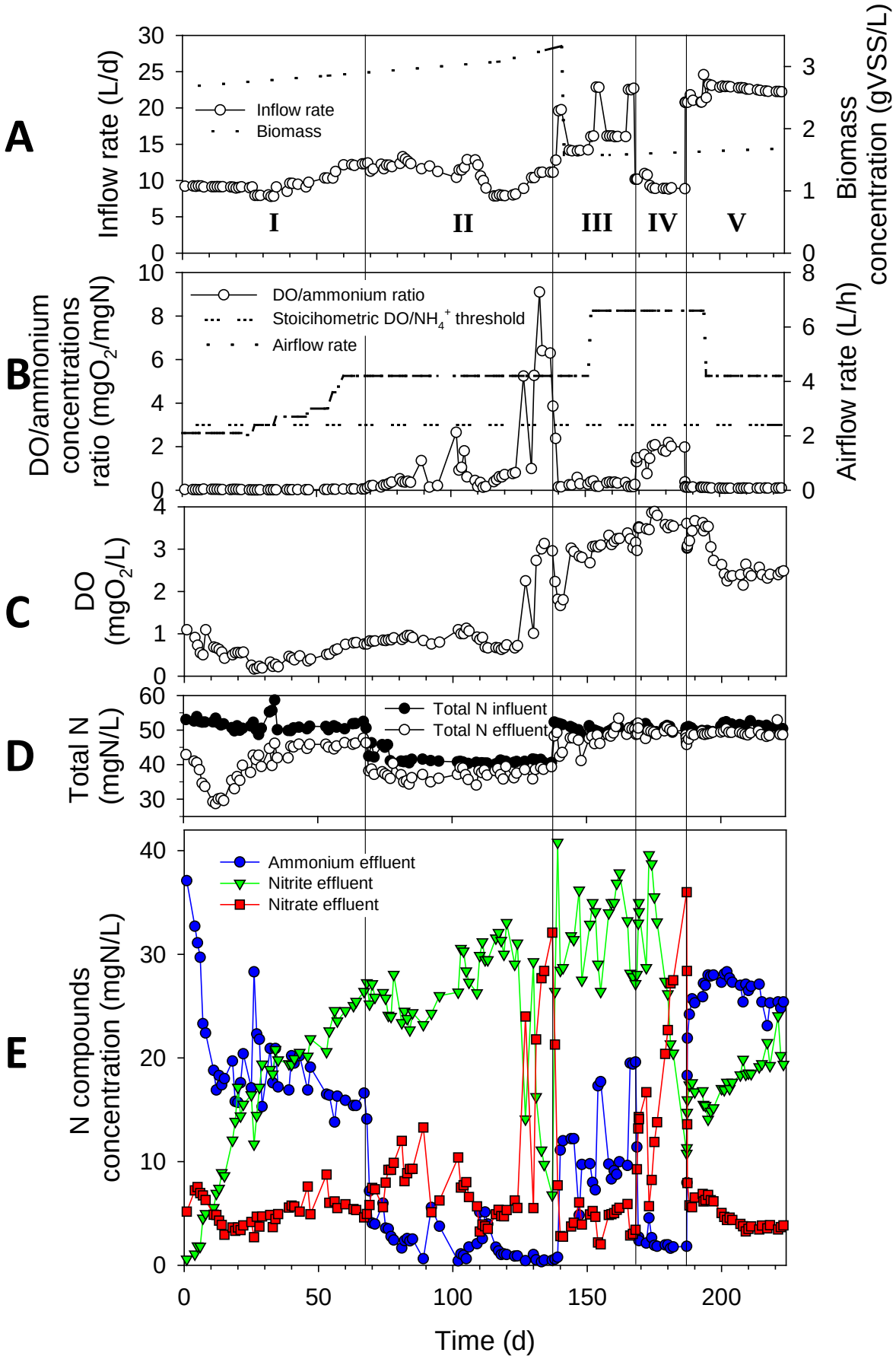
A
Inflow rate (L/d)
Biomass concentration (gVSS/L)
Inflow rate
Biomass
I
II
III
IV
V
B
DO/ammonium concentrations ratio (mgO2/mgN)
Airflow rate (L/h)
DO/ammonium ratio
Stoicihometric DO/NH4+ threshold
Airflow rate
C
DO (mgO2/L)
D
Total N (mgN/L)
Total N influent
Total N effluent
E
N compounds concentration (mgN/L)
Ammonium effluent
Nitrite effluent
Nitrate effluent
Time (d)

Figure 1. Reactor operation. **A**: Inflow rate and biomass concentration. **B**: DO/ammonium concentrations ratio and threshold value indicating when oxygen is the stoichiometrically limiting compound for AOB (see Eq. 2 for details). Airflow applied in the reactor (the superficial air velocity was in the range 3-9 m/h). **C**: Total nitrogen concentration in the inflow and total nitrogen in the effluent. **D**: Ammonium, nitrite and nitrate and DO concentrations in the reactor.

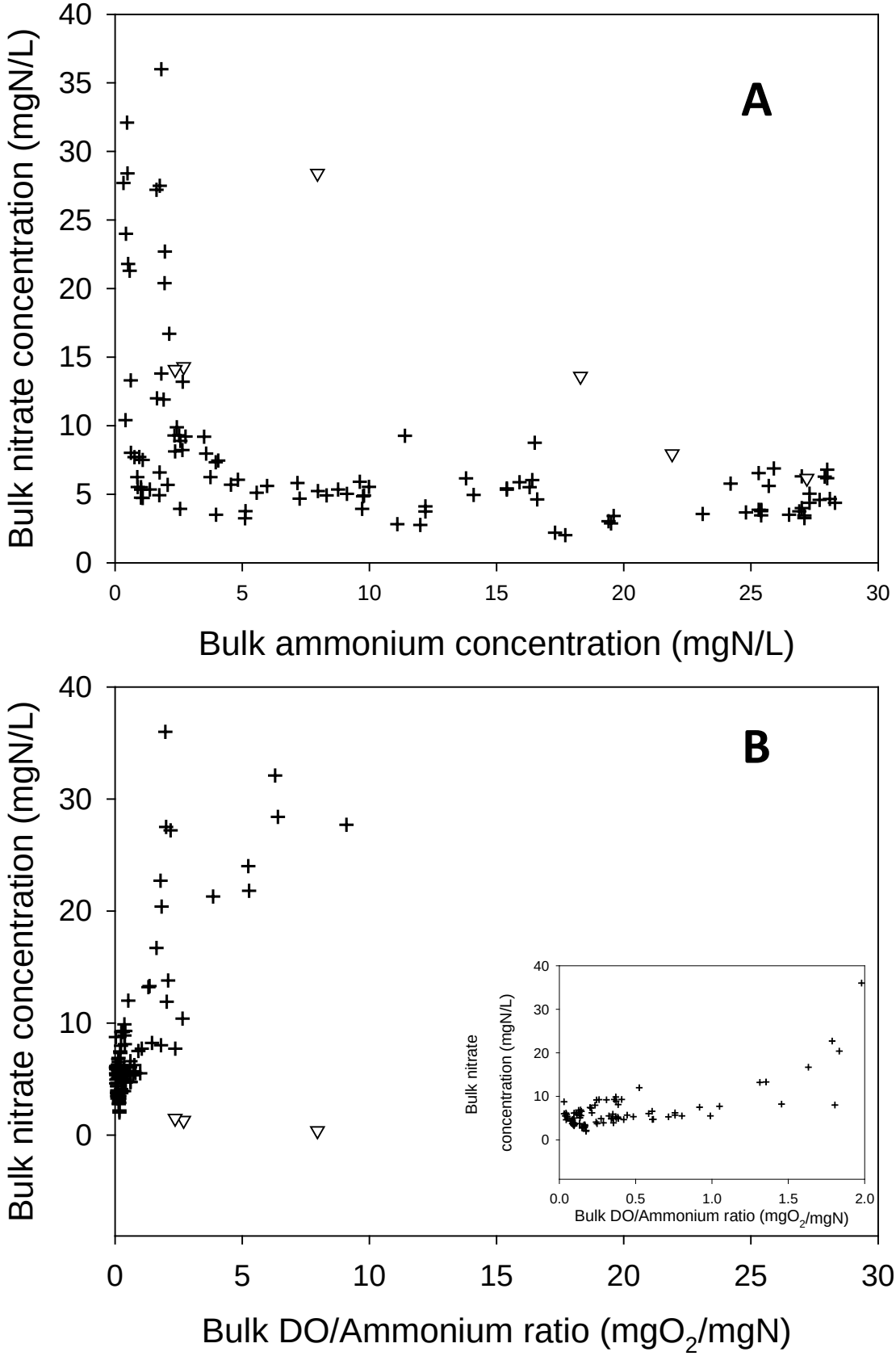

Figure 2. Effluent nitrate concentrations from day 50 onwards correlated with residual ammonium concentration (A) and bulk DO/ammonium concentrations ratio (B). The inset in graph B is a zoomed in version of the main graph, to show variations in the low range of the bulk DO/ammonium concentrations ratio (0-2 g O_2/g N). When the time between

measurements was less than 1 day, the corresponding data were highlighted using triangles, whereas the rest of data points (crosses) were obtained at a slower sampling frequency.

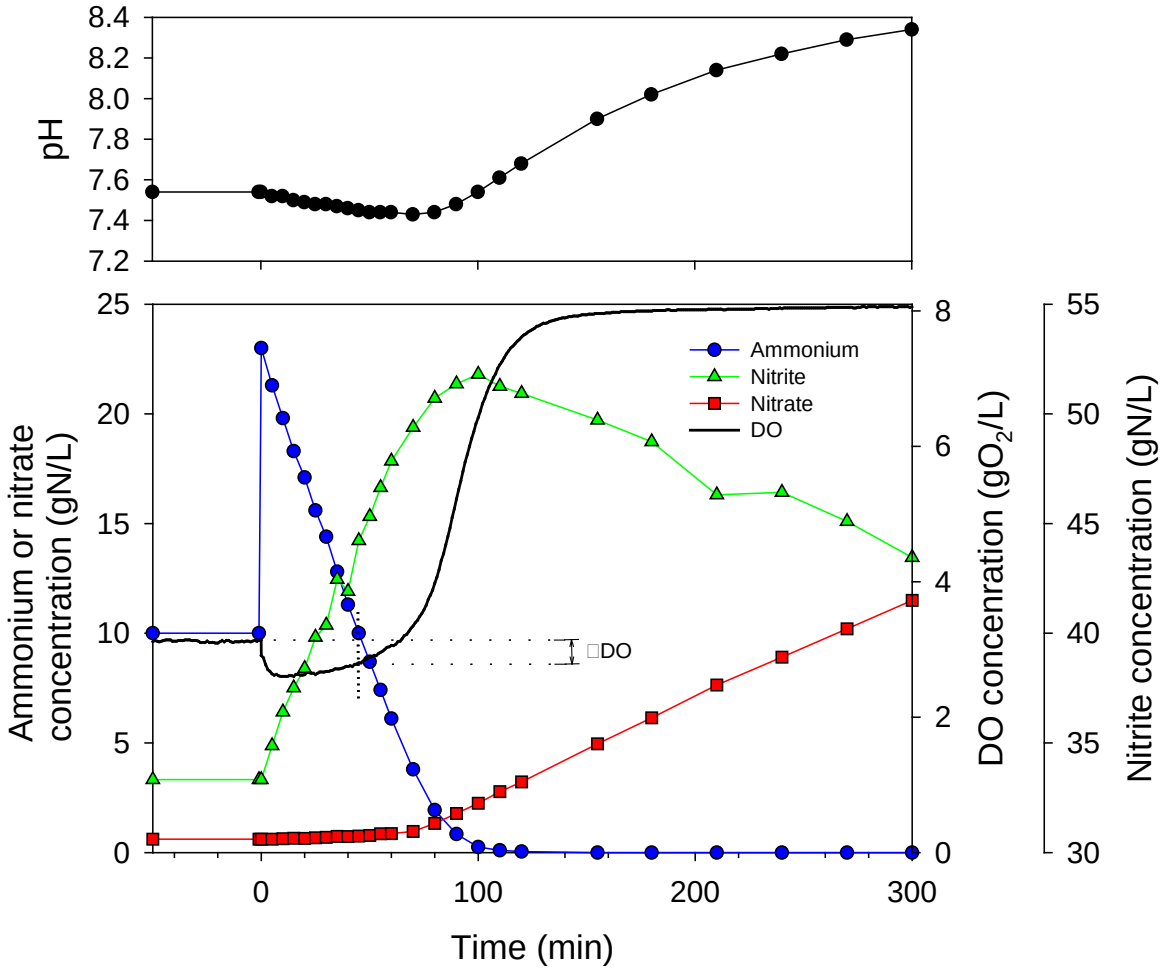

Figure 3. Batch-test performed at day 159 of the operation. An ammonium pulse was added after the inflow rate was stopped (time zero in the graph). The period before time zero indicated the continuous reactor operation before the batch-test. pH was measured but not controlled. The ΔDO highlighted in the figure corresponds to the improved oxygen consumption after the pulse of ammonium, once the bulk ammonium concentration is back to 10 mg N/L (time = 45min).

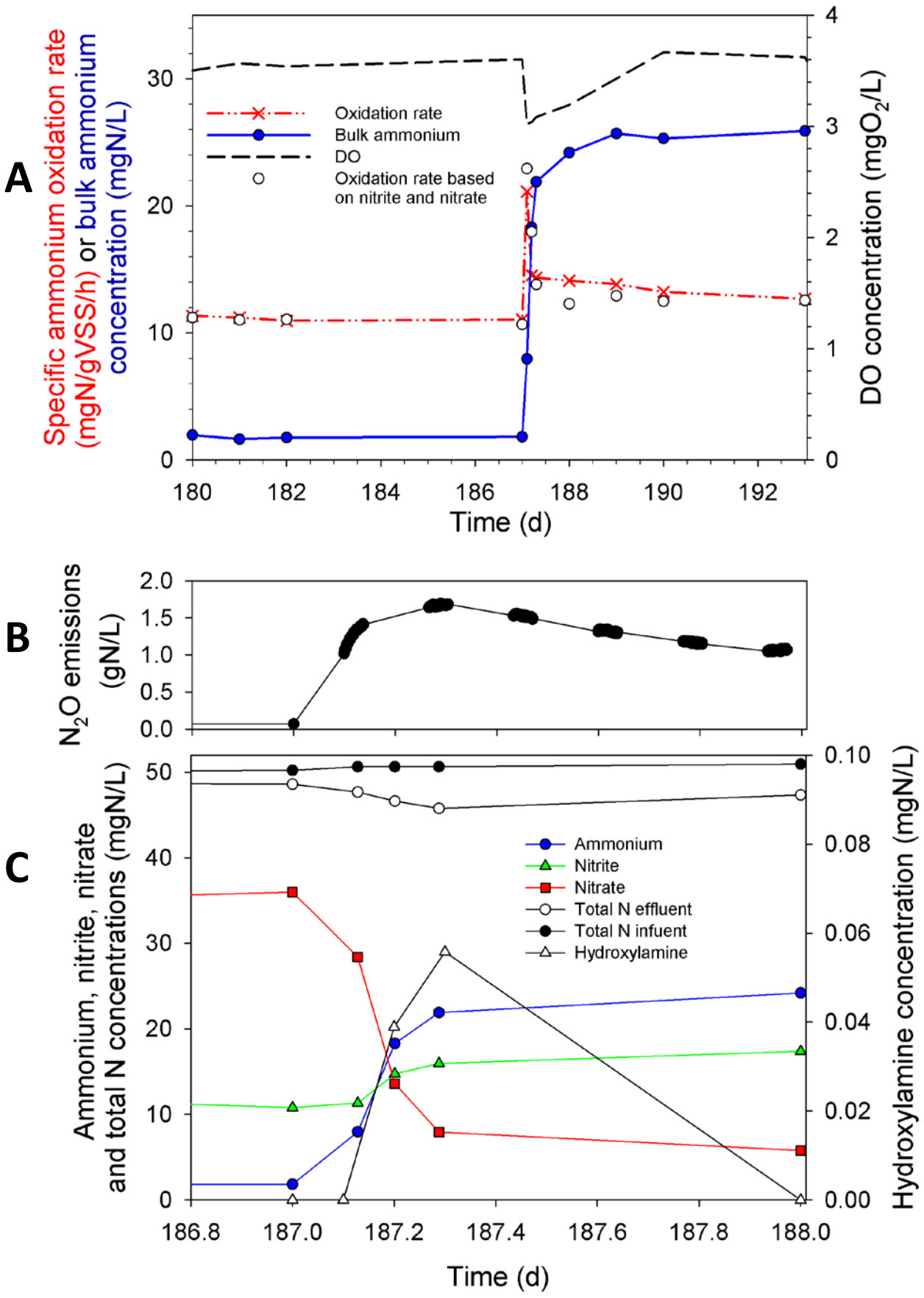

Figure 4. Step-up disturbance in residual ammonium by increasing the flowrate at day 187. **A**: Time course concentrations of ammonium, nitrite and nitrate and hydroxylamine

concentrations. Total nitrogen the influent and effluent has been also included. Specific ammonium oxidation rate has been computed based on the ammonium concentrations (red dashed line) and based on the sum of nitrite and nitrate produced (circles). **B**: N_2O emissions. **C**: Time course bulk ammonium and DO concentration together with the specific ammonium oxidation rate.

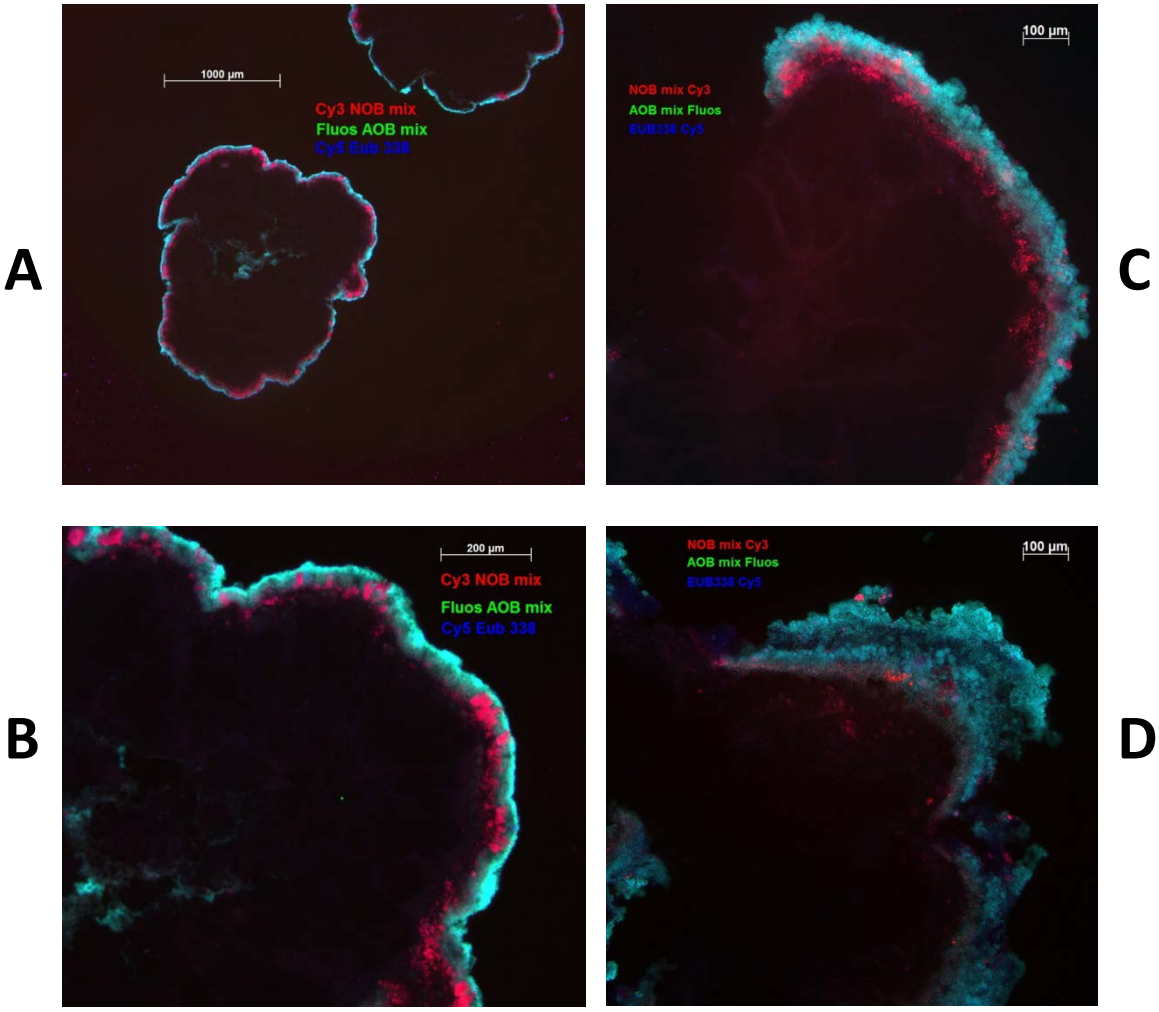

Figure 5. FISH-cryosectioning of granules. Cy3 (red) was used to detect NOB, Fluos (green) to detect AOB and Cy5 (dark blue) to detect most bacteria. Combinations of Cy3 and Cy5 visualised NOB as red/pink and the combination of Fluos and Cy5 visualised AOB as light blue. **A**: Granule slice during period of high residual ammonium concentrations (phase III, day 148)(4x). **B**: Granule slice during period of high residual ammonium concentrations (phase III, day 148, same slice than in Fig. 5A but at 10x magnification).**C**: Granule slice during period of low residual ammonium concentrations (phase V, day 187)(40x). **D**: Granule slice during period of high residual ammonium concentrations (phase V, day 223)(40x).

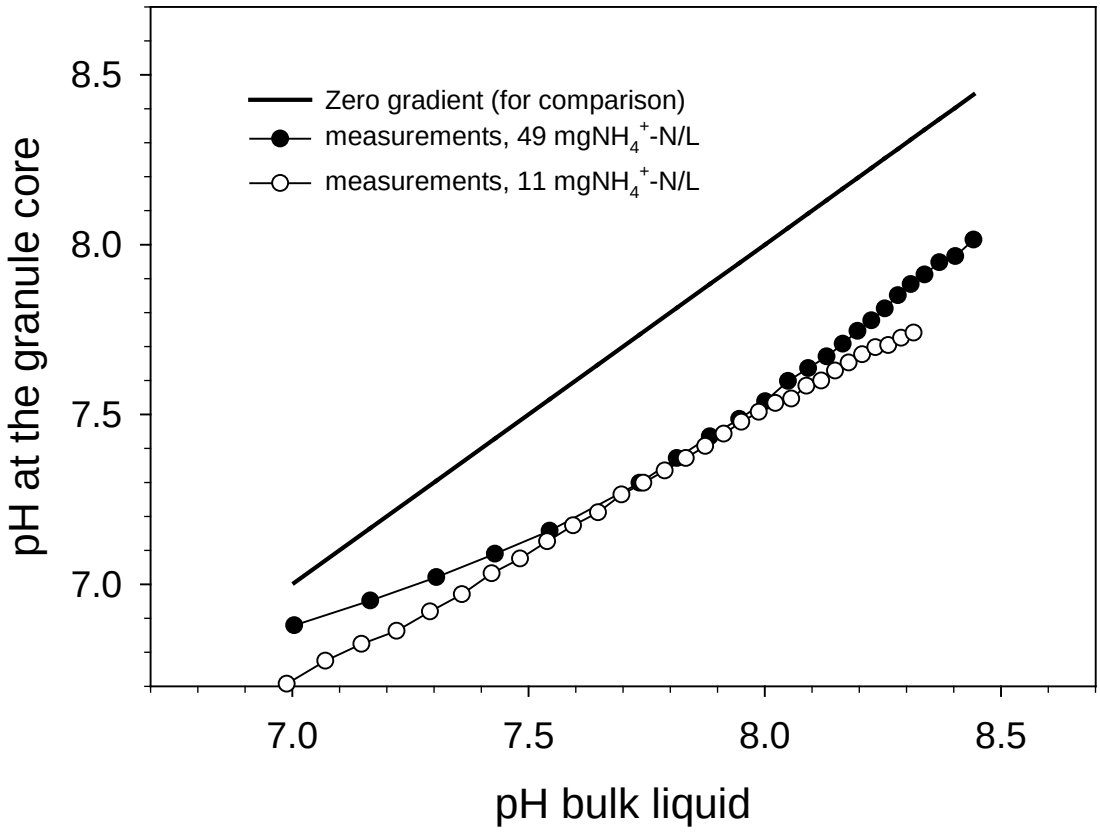

Figure 6. pH difference between the bulk liquid and inside a granule at a bulk pH range of 7.0-8.4. The position for equal pH between the bulk liquid and the granule center has been highlighted by a solid thick line (zero gradient). Points plotted below the grey line indicate a higher pH in the bulk liquid than inside the granule.